algorithms

Article

Performance Evaluation of Daubechies Wavelet-Based Feature Extraction for Multi-State Remaining Useful Life Prediction in Roller Bearings Using Machine Learning Algorithms

Rajkumar Palaniappan

Automation and Sustainability Research Centre (ASRC), Department of Mechatronics Engineering, College of Engineering, University of Technology Bahrain (UTB), Samabad P.O. Box 18041, Bahrain; r.palaniappan@utb.edu.bh; Tel.: +973-39277418

Abstract

Determining the Remaining Useful Life (RUL) in roller bearings is of utmost importance in rotary machinery. Knowing the present state and acting before a failure occurs is the most important aspect in industrial setups. This research presents an effective methodology to determine the RUL state of roller bearings by successfully using different combinations of Daubechies order and decomposition levels of Wavelet Transforms and applying machine learning methods. A dataset comprising temperature and vibration signals collected from a roller bearing test rig was developed for this study. These signals were then filtered using Butterworth bandpass filter for vibration signal filtering and moving average filter for temperature signal filtering followed by splitting the signal into overlapping windows. Then the signals are subjected to Wavelet Packet Transform followed by statistical feature extraction. In the classification phase, machine learning models such as the Support Vector Machine (SVM), K-Nearest Neighbor (KNN), Decision Tree (DT) and Naive Bayes (NB) were used to classify the RUL state in roller bearing. While analyzing different wavelet types (db1 to db10) through seven decomposition levels, this research determined that a db4 wavelet at the third level was identified as optimal for detecting RUL state in roller bearing. The results show that Support Vector Machine (SVM) classifier achieved maximum classification accuracy of 97.68 $\pm$ 0.64%, which is higher than the other classification models used in this study. These results show that the careful calibration of wavelet parameters, combined with an efficient machine learning model can provide a reliable solution for real-time machine health monitoring and predictive maintenance of rotating equipment.

Keywords: roller bearing; remaining useful life (RUL); Daubechies wavelets; machine learning; multi-modal analysis; feature extraction; predictive maintenance; condition monitoring

Academic Editors: Martin Valtierra-Rodriguez, Maximiliano Bueno-Lopez and Afshin Rahimi

Received: 2 June 2026
Revised: 26 June 2026
Accepted: 29 June 2026
Published: 13 July 2026

1. Introduction

The reliability of rotating machinery is the pillar of the modern manufacturing process because if there is any delay due to machine failure, it will affect the production rate, which in turn will affect the production volume. In the manufacturing process, roller bearings are considered the most important yet vulnerable components, as they are exposed to continuous high-speed rotation, varying load conditions, and harsh operational conditions [1]. Based on statistics, bearing-related defects cause nearly 30% to 40% of all mechanical breakdowns in gearboxes and industrial motors [2]. These breakdowns often happen without warning which may lead to secondary damage such as production delays and possible safety risks for workers. Therefore, the transition from conventional preventive maintenance to a data-driven predictive maintenance (PdM) approach has become an important objective in the age of Industry 5.0 [3].

The fundamental need of a PdM system is to determine the Remaining Useful Life (RUL) of industrial machines or components to avoid before failure occurs [4]. RUL provides a time frame that defines the remaining operational time of a component before it reaches a failure [5]. By correctly predicting RUL, maintenance engineers or technicians can move away from "run-to-failure" models and implement intervention schemes based on the actual condition of the component or equipment. Determining the RUL of machine component is challenging because the vibration signals are too complex in nature. Vibration signals collected from a degrading roller bearing are non-linear, non-stationary, and affected by acoustic emissions from various sources [6].

Recent developments in the field of Artificial Intelligence (AI) have provided powerful tools to overcome the complex nature of vibration signals [7]. Conventional methods are difficult to create because an expert who understands how materials wear out due to various factors is required [8]. However, machine learning models learn degradation patterns directly from historical sensor data without explicit physical modeling. However, the model performance remains fundamentally constrained by the quality of input data and the feature extraction method. Most existing machine learning algorithms find it hard to obtain high classification accuracy across the complete lifespan of a bearing, often failing to classify early-stage to late-stage RUL [9].

The aim of this research is to implement an RUL state prediction for roller bearings that uses the Daubechies wavelet to extract features. The exact frequency ranges where indications of a roller bearing degradation are easily found can be determined by decomposing the raw vibration and temperature signals into multiple levels of resolution using WPT. Unlike conventional approaches, this research conducts a systematic investigation into the impact of wavelet orders (db1–db10) and decomposition levels (1–7) on RUL state in roller bearings. By modeling the problem as a five state RUL classification (15%, 25%, 50%, 75%, 100% RUL) in roller bearings, this research presents a more specific and actionable roller bearing condition indicator than conventional binary fault indicators.

2. Literature Review

The search for previous research on RUL estimation methodology has resulted in a range of AI-based methods. Early methods focused on time-domain statistical features from raw signals. The work of Huang et al. [10] combined statistical features such as Root Mean Square (RMS), Kurtosis, and Crest Factor along with self-organizing maps to classify faults in roller bearings, and the results indicated that there was a notable margin of error. Similarly, the work of Chen et al. [11] applied Gaussian Mixture Models (GMM) by fusing vibration data with electrostatic wear-site data, showing that multi-sensor fusion can improve RUL prediction more effectively. The effectiveness of time-domain features is often weakened during a bearing's intermediate degradation stages, as feature values stabilize and fail to reflect ongoing wear which leads to unreliable RUL estimation.

To overcome these limitations, researchers moved toward frequency domain and time-frequency domain signal analysis. The work of Castejón et al. [12] applied Discrete Wavelet Transforms (DWT) with Multilayer Perceptron (MLP) neural network and reported a maximum classification accuracy of 85% for their model. Regardless of the benefits of DWT, many researchers found that the feature set is high in dimensions, which requires appropriate management. Therefore, Principal Component Analysis (PCA) or similar dimensionality reduction techniques became a standard preprocessing stage in research that uses WPT. In the work of Sun et al. [13] PCA-based feature reduction and SVM classification model were used and it was found that this method reduces the error to less than 4%, while the work of Kim et al. [14] expanded the feature pool to include entropy estimation and shape factors, reaching a maximum classification accuracy of 94.4% in detecting RUL in bearings.

The combinations of advanced probability functions and hybrid AI models have also been explored in RUL detection in roller bearings. The work of Tian et al. [15] used a Generalized Weibull-FR function within an Artificial Neural Network (ANN) classifier to model RUL in bearing. In the work of Medjaher et al. [16], speed and load variation were focused on using a mixture of Gaussians Hidden Markov Models, although the reported classification accuracy remained relatively low, which is almost 78%. Ben et al. [17] achieved nearly 99% classification accuracy for the "normal" class using simplified Fuzzy adaptive resonance theory but particularly observed a substantial reduction in classification accuracy when trying to classify specific stages of degradation, which is a common bottleneck in multi-state RUL classification in roller bearings.

Deep Learning (DL) has lately overshadowed literature by removing the need for manual feature engineering. The work of Ren et al. [18] applied Deep Neural Networks (DNNs) and attained RMSE values close to zero on standard datasets, while Deutsch et al. [19] and Ren et al. [20] applied Restricted Boltzmann Machines and Deep Convolutional Neural Networks (DCNNs) to the IEEE PHM2012 challenge dataset, and obtained highly precise error margins. The work of Cheng et al. [21] and Lu et al. [22] applied Generative Adversarial Networks (GANs) and Long Short-Term Memory (LSTM) models to capture the temporal dependencies of degradation in roller bearings. While Deep Learning models like those in the works of [23,24] achieve RUL classification accuracy near 99%, they often require substantial computing capability and extensive data [24], making it difficult to implement in real-time, low-power industrial edge devices.

Even though there is progress in the field of RUL classification in bearings, a critical gap remains in the choice of wavelet parameters. In the year 2023, the works of Kumar et al. [25] and Motahari et al. [26] applied Wavelet Transforms and reported a classification accuracy of almost 83.3%. This indicates that simply applying a Wavelet Transform is not sufficient. A detailed analysis of different parameters might improve the results further. Most research uses "default" wavelet without justifying its choice over other orders or investigating the optimal level of decomposition. Furthermore, while models used in the work of [27,28] show high accuracy for SVM and XGBoost respectively, these studies do not explore how the primary feature extraction method directly affects the classifier's capability to separate neighboring RUL states. Existing research has demonstrated promising results for bearing condition assessment; however, many depend on either vibration signal or limited fault categories, or it is a binary classification problems or computationally intensive deep learning models. These limitations aid the development of an efficient multi-modal feature-based machine learning model for bearing condition monitoring. This study addresses the identified gap by conducting a detailed analysis of the different Daubechies order and decomposition levels. This study establishes strong evidence between wavelet selection and multi-state RUL classification in roller bearing.

3. Methodology

This study uses a systematic process to classify the RUL state in roller bearings using signal processing techniques and machine learning models and compares the results. First the temperature and vibration signals were collected from the roller bearing test rig followed by filtering the signals. Then the signals are subject to overlapping and windowing followed by wavelet packet transformation to extract statistical features. The extracted features are then reduced in dimension using Principal Component Analysis (PCA). Lastly, machine learning models are used to accurately identify if the bearings are RUL state. The proposed framework for RUL state classification in roller bearing is shown in Figure 1.

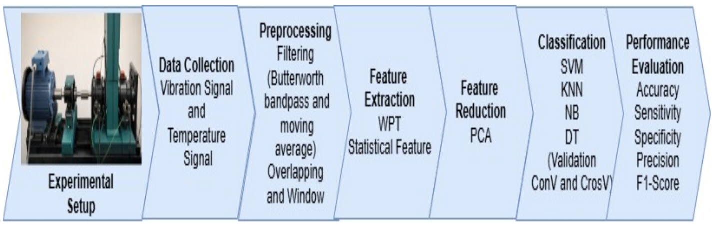

Figure 1. RUL state classification framework.

The data for this study were collected from a custom-built roller bearing test rig at the GDR TECH industry. This study utilizes piezoelectric accelerometers for vibration signals with a sampling rate of 25.6 kHz and K-type thermocouples for temperature signals with a sampling rate of 1 kHz for data collection. Each raw signal sample lasts for a duration of 10 s. The data was collected from a test rig consisting of an AC motor-driven shaft supporting an industrial roller bearing (Model NU205; bore diameter 25 mm, outer diameter 52 mm, width 15 mm) under a constant radial load of 5 kN and a fixed speed of 1450 RPM, with failure defined as the condition in which vibration levels surpassed a peak acceleration of 20 m/s^2 or housing temperature exceeded 75 °C. While these hard thresholds are used as emergency criteria to terminate the physical experiment, a machine learning framework is essential to track the complex and non-linear degradation pattern and predict the Remaining Useful Life (RUL) hours before these extreme operational conditions are reached. The resulting dataset contains 5000 measurement samples, divided into five balanced classes of 1000 samples each representing the RUL states 15%, 25%, 50%, 75%, and 100% (Healthy). The RUL state classes were categorized as 0–15% as 15% class, 16–25% as 25% class, 26% to 50% as 50% class, 51% to 75% as 75% class and 76% to 100% as 100% class. The 100% RUL signifies a brand-new component with its full life remaining, while 0% RUL signifies failure. These RUL state classes were verified based on a run-to-failure protocol, where the total operational life of the roller bearing was back calculated into RUL percentage states to verify accurate labeling of RUL states in roller bearing. The labeling of RUL state was done based on back-calculation of RUL percentage from the total operational time during the experiment. Specifically, once the total operational life (*Ttotal*) of the bearing was known at the end of the run-to-failure test, the RUL percentage at any measurement time t was computed using Equation (1).

$$RUL\ \% = \left(\frac{Ttotal - t}{T_{total}}\right) \times 100 \quad (1)$$

The raw signal data was subjected to distinct denoising techniques for vibration and temperature signals respectively. The vibration signals were filtered by implementing a 4th-order Butterworth band-pass filter with a pass band of [2 kHz–10 kHz] which isolates the high-frequency structural resonances and suppress electrical noise. For the temperature signals moving average (MA) filter with a window size of M = 30 was used to filter out stochastic measurement jitter in the signal. Following the filtering stage, a sliding window approach with 50% overlap was implemented to segment the signal, which enhances the temporal continuity and improves the feature density. The feature extraction stage was initiated on windowed temperature and vibration signals using one-to-seven decomposition-level Wavelet Packet Transform (WPT) across individual Daubechies mother wavelets (db1 to db10). The Wavelet Packet Transform (WPT) with a Daubechies (db1–db10) mother wavelets and decomposition levels ranging from levels 1 to 7 was selected in this research to decompose both low- and high-frequency bands uniformly into multi-scale, high-resolution sub-bands [29]. The db family was specifically chosen over other wavelet families because its mathematical orthogonality prevents feature data redundancy, while its asymmetric geometry and maximal vanishing moments offer an optimal structural match for isolating sharp, transient bearing impact pulses and early-stage degradation harmonics from background noise [30]. This method returned variable terminal sub-bands which capture energy shifts within the frequency spectrum. From these sub-bands from the filtered segments, four statistical features were extracted from vibration signal are Root Mean Square (RMS) for energy intensity, Kurtosis for signal impulsiveness, Crest Factor for peak severity, and Relative Energy. Similarly, two statistical features were extracted from the temperature signals, namely mean temperature and standard deviation. These features were selected because they track distinct stages of physical damage, an approach well established in bearing prognosis literature [31]. As verified by previous studies, overall energy parameters like RMS and temperature track late-stage structural wear, whereas dimensionless parameters like Kurtosis and Crest Factor are highly sensitive to sudden, sharp impact shocks, allowing for early defect detection [32]. The mathematical formula for these features is shown in Table 1.

Table 1. Statistical features extracted from both temperature and vibration signals.

Feature Category	Statistical Feature	Abbreviation	Formula	Variable Descriptions
Vibration Signal	Root Mean Square	RMS	$\sqrt{\frac{1}{N}\sum_{i=1}^{N} x_i^2}$	x_i: discrete vibration amplitude values N: total number of vibration samples in the window
	Kurtosis	K	$\frac{\frac{1}{N}\sum_{i=1}^{N}(x_i-\overline{x})^4}{\left(\frac{1}{N}\sum_{i=1}^{N}(x_i-\overline{x})^2\right)^2}$	$\overline{x}$: mean value of the vibration signal
	Crest Factor	CF	$\frac{\max\lvert x_i\rvert}{\mathrm{RMS}}$	$\max\lvert x_i\rvert$: absolute peak value of the vibration signal
	Relative Energy	RE	$\frac{E_{sub-band}}{E_{total}} \times 100\%$	$E_{sub-band}$: energy calculated within a specific WPT node E_{total}: total energy across all WPT nodes in the window
Temperature Signal	Mean Temperature	$\overline{T}$	$\frac{1}{M}\sum_{j=1}^{M} T_j$	T_j: discrete temperature reading values M: Total number of temperature samples in the window
	Standard Deviation	SD	$\sqrt{\frac{1}{M-1}\sum_{j=1}^{M}(T_j-\overline{T})^2}$	$\overline{T}$: mean value of the temperature signal

At decomposition level L, WPT creates 2^L terminal nodes. For each node, RMS, Kurtosis, Crest Factor, and Relative Energy were obtained from each segmented window. Therefore, the vibration feature dimension can be expressed as

$$D_v = 4 \times 2^L \tag{2}$$

Two temperature-domain features (mean temperature and standard deviation) were extracted from each segmented window

$$D_t = 2 \times 2^L \tag{3}$$

Therefore, the total feature dimension per segmented window before PCA becomes:

$$D_{total} = 6\,(2^L) \tag{4}$$

Accordingly, feature dimensions ranged from 12 features at decomposition Level 1 to 768 features at decomposition Level 7 per segmented window. The feature dimensionality at different decomposition levels along with the feature extraction time per window is provided in Table 2.

Principal Component Analysis (PCA) was applied to simplify the data by turning the original features into a few new, independent columns, keeping only the ones that hold 95% of the important information. Each configuration of Daubechies wavelet order and decomposition level was tested separately as a unique input for the machine learning models. The final phase involves classification of RUL stages in roller bearing using four standard machine learning algorithms, namely Support Vector Machine (SVM), K-Nearest Neighbors (KNN), Decision Tree (DT), and Naive Bayes (NB). These four classification models were used to ensure that a robust and comprehensive evaluation of the roller bearing RUL state estimation is done. To ensure optimal classification performance, the hyperparameters for the models were established using a grid-search cross-validation approach: the Support Vector Machine (SVM) utilized a Radial Basis Function (RBF) kernel with optimized box constraint ($C = 1.0$) and kernel scale ($\gamma = 0.1$) parameters, the K-Nearest Neighbors (KNN) model was configured with $K = 5$ using Euclidean distance, and the Decision Tree (DT) was bounded by a maximum tree depth of 10 to balance model accuracy against the risk of overfitting. The Naive Bayes (NB) classifier was implemented using a Gaussian distribution with class priors estimated from the training data and a variance smoothing parameter of 1×10^{-9}. To ensure machine learning model generalizability and overcome overfitting, both conventional validations using 70/30 data splits with random 10 seeds, and 10-fold cross-validation with random 10 seeds were used in this research and mean $\pm$ standard deviation (SD) are reported in this study. The RUL state classification in roller bearing was computed through various performance metrics such as accuracy, sensitivity, specificity, precision, and F1-Score, providing a statistically comprehensive evaluation of the model's classification ability across different RUL states in roller bearings.

Table 2. Feature dimensionality at different decomposition levels.

Decomposition Level (L)	Terminal Nodes (2^L)	Vibration Features	Temperature Features	Total Features	Feature Extraction Time per Window in ms
1	2	8	4	12	1.2 ± 0.2
2	4	16	8	24	2.1 ± 0.3
3	8	32	16	48	3.8 ± 0.4
4	16	64	32	96	7.2 ± 0.6
5	32	128	64	192	14.5 ± 1.1
6	64	256	128	384	29.3 ± 2.3
7	128	512	256	768	58.6 ± 4.1

4. Results and Discussion

This section provides a detailed analysis of the classification accuracy of the proposed RUL state classification method for roller bearings, focusing on the comparative analysis of the performance of 10 Daubechies wavelet orders (db1–db10) and 7 decomposition levels. A total of 5000 balanced samples representing five distinct RUL states (15%, 25%, 50%, 75%, and 100% RUL state) were processed through the Wavelet Packet Transform (WPT). The extracted statistical feature vectors were dimensionally reduced using PCA and fed across four supervised learning models, namely SVM, KNN, DT, and Naive Bayes, using both conventional training and cross-validation schemes. The resulting analysis investigates the critical comparison between wavelet smoothness and temporal resolution which identifies the ideal feature parameters for RUL stage classification in roller bearing. By examining accuracy, sensitivity, and F1-scores, this discussion establishes the mathematical justification for the superior performance of the specific db and Level configuration and demonstrates its robustness in distinguishing between RUL stages in roller bearings.

Table 3 shows the performance evaluation of the four classification models with different db and levels of decomposition. The conventional validation of data split 70:30 is denoted as Conv, and the 10-fold cross-validation is denoted as Cros in the Table. As shown in Table 3, feature extraction performance reaches the highest classification accuracy and then declines based on the chosen wavelet parameters. The maximum classification accuracy of 97.68 $\pm$ 0.64% was achieved by the SVM classifier with db4 and Level 3 feature set. At this db wavelet selection and decomposition level, the wavelet support associates with the characteristic fault frequency of the respective roller bearing RUL stage. When assessing the Daubechies orders, it becomes apparent that db1 to db3 lack the mathematical "smoothness" required to overlap with the curvilinear characteristics of the temperature and vibration signals, indicating higher residual noise in the coefficients. On the other hand, higher orders from db5 to db10 increase the number of vanishing moments; while this increases frequency localization, the subsequent increase in computational filter size which causes a "blurring" of the time-domain transients. This is analytically exhibited in the SVM model's performance, which steadily decreases from its 97.68% peak classification accuracy at db4 to 89.0% at db10, demonstrating that excessive mathematical complexity in the end compromises the classification accuracy sharply due to impulsive degradation events.

The effect of the decomposition level (1–7) is increasingly evident compared to the wavelet order, acting as the fundamental factor for class separability. In decomposition levels 1 and 2, the feature domain is full of high-frequency spectral components and transducer noise, causing the Naive Bayes and Decision Tree classifiers to have classification accuracy close to 75–80%, which is quite low. Moving on to Level 3 decomposition which acts as a band-pass filter that splits the primary energy of the bearing's structural resonance. Even the less robust Naive Bayes classifier experiences a significant performance improvement to 92.2% at this level. This suggests that the quality of the feature at this level is fundamentally better and more efficient. However, as the analysis proceeds to the higher decomposition levels 5, 6, and 7, the signal is subjected to continuous reduction in data and low-pass filtering. This process effectively removes the high-frequency artifacts that distinguish the RUL states, resulting in high-dimensional feature space where the classification model can no longer maintain clear decision boundaries. Figure 2 shows the heatmap for Cros and Conv data from Table 3. In comparison between both the Conv and Cros validation methods, the conventional validation method performed well which is evident from both Table 3 and Figure 2. To prove how the wavelet choices affect the results, we tested different settings using two validation methods in Figure 2. The left plot shows 10-fold cross-validation (crosv), and the right plot shows the conventional 70:30 split (conv). Both plots show the exact same trend: the highest accuracy happens exactly at db4 with a decomposition level of 3. If we look vertically at higher-order wavelets (from db5 to db10), the accuracy drops down significantly. This suggests that longer wavelet filters smooth out and 'blur' the sharp vibration spikes (transients) needed to find faults. Similarly, if we look horizontally past Level 3 toward deeper levels (4 to 7), the accuracy drops steadily. This confirms that splitting the signal too many times introduces noise and reduces class separability, making the states harder to classify. The db4 wavelet at Level 3 decomposition works best because its 8-tap filter length matches the physical duration of bearing fault impacts, while splitting the data into 8 frequency bands directly aligns with the natural resonance frequencies caused by bearing defects [33]. As verified empirically in Figure 2, this configuration prevents structural blurring and preserves maximum class separability. The conventional validation reached maximum classification accuracy around 97.68% and cross-validation was slightly less with 95% classification accuracy for SVM classifier.

Table 3. Performance comparison of wavelet-based feature extraction across multiple classifiers and decomposition levels.

db N—Daubechies Order	Classifier	Decomposition Level													
		1		2		3		4		5		6		7	
		Conv	Cros	Conv	Cros	Conv	Cros	Conv	Cros	Conv	Cros	Conv	Cros	Conv	Cros
db1	DT	76.2 ± 0.4	75.8 ± 0.3	78.4 ± 0.6	76.5 ± 0.8	80.1 ± 0.5	77.9 ± 0.5	78.8 ± 0.7	76.2 ± 0.4	77.1 ± 0.6	76.0 ± 0.2	76.3 ± 0.5	75.5 ± 0.4	76.0 ± 0.4	75.9 ± 0.3
	NB	75.8 ± 0.4	75.9 ± 0.3	76.6 ± 0.9	76.1 ± 0.7	77.4 ± 0.4	75.9 ± 0.4	76.1 ± 0.4	75.4 ± 0.4	75.9 ± 0.4	75.2 ± 0.4	75.9 ± 0.4	75.8 ± 0.4	76.0 ± 0.5	75.8 ± 0.4
	KNN	81.1 ± 0.6	79.2 ± 0.6	83.1 ± 0.7	81.1 ± 0.6	85.2 ± 0.6	83.4 ± 0.5	83.9 ± 0.6	81.3 ± 0.4	82.1 ± 0.4	80.3 ± 0.8	81.6 ± 0.7	79.2 ± 0.4	79.0 ± 0.5	77.2 ± 0.6
	SVM	88.3 ± 0.5	86.4 ± 0.6	90.8 ± 0.5	88.4 ± 0.6	92.7 ± 0.6	90.0 ± 0.5	91.3 ± 0.7	89.3 ± 0.8	89.0 ± 0.6	87.2 ± 0.5	88.2 ± 0.6	86.6 ± 0.6	86.9 ± 0.5	85.4 ± 0.8
db2	DT	76.4 ± 0.4	76.1 ± 0.4	79.0 ± 0.6	77.2 ± 0.6	81.0 ± 0.6	78.0 ± 0.6	79.1 ± 0.4	77.3 ± 0.4	78.6 ± 0.5	77.6 ± 0.4	77.9 ± 0.4	76.6 ± 0.3	76.6 ± 0.4	75.8 ± 0.4
	NB	75.9 ± 0.4	75.8 ± 0.3	77.0 ± 0.3	76.3 ± 0.4	78.2 ± 0.8	76.7 ± 0.6	77.7 ± 0.4	76.4 ± 0.4	77.5 ± 0.5	76.4 ± 0.4	76.1 ± 0.4	76.1 ± 0.4	75.8 ± 0.4	75.9 ± 0.3
	KNN	86.0 ± 0.6	84.4 ± 0.6	88.1 ± 0.7	85.2 ± 0.7	88.9 ± 0.6	86.9 ± 0.7	88.4 ± 0.6	86.7 ± 0.6	88.1 ± 0.6	85.8 ± 0.6	87.2 ± 0.6	85.9 ± 0.6	84.5 ± 0.6	82.1 ± 0.6
	SVM	86.8 ± 0.6	85.2 ± 0.6	89.6 ± 0.6	87.8 ± 0.7	90.9 ± 0.6	89.0 ± 0.5	89.7 ± 0.6	88.3 ± 0.6	89.2 ± 0.6	88.5 ± 0.7	88.4 ± 0.6	87.0 ± 0.5	87.7 ± 0.5	85.7 ± 0.6
db3	DT	77.0 ± 0.6	76.1 ± 0.4	80.1 ± 0.4	78.8 ± 0.5	81.6 ± 0.5	79.0 ± 0.6	80.4 ± 0.5	79.0 ± 0.4	79.2 ± 0.4	78.4 ± 0.4	78.8 ± 0.4	77.8 ± 0.4	77.8 ± 0.4	76.6 ± 0.5
	NB	76.2 ± 0.4	75.9 ± 0.4	77.9 ± 0.5	76.4 ± 0.4	78.9 ± 0.6	77.2 ± 0.6	78.3 ± 0.4	76.8 ± 0.4	77.0 ± 0.5	76.2 ± 0.4	76.6 ± 0.6	75.9 ± 0.4	76.0 ± 0.6	75.9 ± 0.5
	KNN	84.0 ± 0.6	81.4 ± 0.6	86.1 ± 0.6	84.4 ± 0.6	88.0 ± 0.7	85.7 ± 0.6	86.6 ± 0.6	84.8 ± 0.6	85.5 ± 0.6	83.6 ± 0.6	84.4 ± 0.6	82.4 ± 0.6	83.8 ± 0.4	81.5 ± 0.5
	SVM	86.1 ± 0.6	83.5 ± 0.6	88.1 ± 0.6	85.2 ± 0.6	89.5 ± 0.6	87.6 ± 0.6	88.9 ± 0.7	87.1 ± 0.7	88.5 ± 0.6	86.6 ± 0.6	88.0 ± 0.6	85.1 ± 0.7	85.0 ± 0.6	83.4 ± 0.6

Table 3. *Cont.*

db4	DT	82.4 ± 0.6	80.1 ± 0.7	89.0 ± 0.6	87.2 ± 0.6	94.0 ± 0.6	91.0 ± 0.6	88.1 ± 0.8	85.3 ± 0.9	84.6 ± 0.5	81.6 ± 0.8	82.9 ± 0.8	80.6 ± 0.7	78.6 ± 0.8	76.8 ± 0.4
	NB	80.9 ± 0.4	78.8 ± 0.3	87.0 ± 0.7	85.3 ± 0.8	92.2 ± 0.8	89.7 ± 0.6	86.7 ± 0.6	84.4 ± 0.8	81.5 ± 0.5	79.4 ± 0.5	78.1 ± 0.6	76.1 ± 0.5	75.8 ± 0.4	75.9 ± 0.3
	KNN	86.0 ± 0.6	84.4 ± 0.6	90.1 ± 0.7	88.2 ± 0.7	95.9 ± 0.6	93.9 ± 0.7	90.4 ± 0.6	88.7 ± 0.6	89.1 ± 0.6	86.8 ± 0.6	87.2 ± 0.6	85.9 ± 0.6	84.5 ± 0.6	82.1 ± 0.6
	SVM	89.8 ± 0.6	87.2 ± 0.6	92.6 ± 0.6	90.8 ± 0.7	97.68 ± 0.64	95.0 ± 0.5	93.7 ± 0.6	91.3 ± 0.6	92.2 ± 0.6	90.5 ± 0.7	89.4 ± 0.6	87.0 ± 0.5	87.7 ± 0.5	85.7 ± 0.6
db5	DT	79.1 ± 0.4	77.3 ± 0.4	82.0 ± 0.4	80.0 ± 0.4	82.5 ± 0.5	79.5 ± 0.5	84.3 ± 0.5	82.2 ± 0.4	83.6 ± 0.4	82.0 ± 0.4	80.9 ± 0.4	78.3 ± 0.4	79.0 ± 0.5	76.2 ± 0.5
	NB	76.1 ± 0.4	75.9 ± 0.4	76.5 ± 0.4	76.0 ± 0.5	77.8 ± 0.5	75.9 ± 0.4	78.8 ± 0.4	77.0 ± 0.5	77.2 ± 0.4	75.9 ± 0.4	76.1 ± 0.4	75.8 ± 0.3	75.9 ± 0.4	75.9 ± 0.4
	KNN	83.8 ± 0.4	81.1 ± 0.4	86.8 ± 0.4	85.0 ± 0.5	88.5 ± 0.4	86.0 ± 0.5	89.0 ± 0.4	87.1 ± 0.5	88.7 ± 0.5	86.7 ± 0.4	87.3 ± 0.5	85.2 ± 0.4	84.5 ± 0.5	81.6 ± 0.4
	SVM	88.3 ± 0.5	86.5 ± 0.4	90.8 ± 0.4	89.2 ± 0.5	91.9 ± 0.4	90.4 ± 0.5	91.6 ± 0.4	89.8 ± 0.5	91.5 ± 0.5	90.5 ± 0.4	89.3 ± 0.5	87.1 ± 0.4	87.5 ± 0.4	85.1 ± 0.5
db6	DT	78.2 ± 0.5	76.4 ± 0.4	81.1 ± 0.4	79.2 ± 0.5	82.9 ± 0.4	80.1 ± 0.5	83.4 ± 0.5	81.1 ± 0.4	82.6 ± 0.4	80.4 ± 0.4	79.8 ± 0.4	77.5 ± 0.4	78.1 ± 0.4	76.0 ± 0.4
	NB	75.9 ± 0.4	75.8 ± 0.4	76.3 ± 0.4	76.0 ± 0.4	77.2 ± 0.4	75.9 ± 0.3	78.1 ± 0.4	76.5 ± 0.4	76.9 ± 0.4	75.8 ± 0.3	76.0 ± 0.4	75.8 ± 0.3	75.8 ± 0.4	75.8 ± 0.3
	KNN	82.7 ± 0.4	80.3 ± 0.4	85.9 ± 0.4	84.1 ± 0.4	87.1 ± 0.4	85.0 ± 0.4	88.4 ± 0.4	86.5 ± 0.4	87.9 ± 0.5	85.8 ± 0.4	86.1 ± 0.4	84.3 ± 0.4	83.6 ± 0.4	81.0 ± 0.4
	SVM	87.5 ± 0.5	85.6 ± 0.4	89.9 ± 0.4	88.1 ± 0.5	91.2 ± 0.4	89.4 ± 0.4	90.8 ± 0.4	89.1 ± 0.4	90.7 ± 0.5	88.9 ± 0.4	88.6 ± 0.5	86.5 ± 0.4	86.9 ± 0.4	84.4 ± 0.4
db7	DT	77.5 ± 0.5	76.1 ± 0.4	80.4 ± 0.4	78.5 ± 0.5	82.1 ± 0.4	79.6 ± 0.4	82.7 ± 0.5	80.4 ± 0.4	81.8 ± 0.4	79.7 ± 0.4	79.1 ± 0.4	76.8 ± 0.4	77.5 ± 0.5	75.9 ± 0.4
	NB	75.8 ± 0.4	75.8 ± 0.3	76.2 ± 0.4	75.9 ± 0.4	76.9 ± 0.4	75.8 ± 0.3	77.6 ± 0.4	76.1 ± 0.4	76.4 ± 0.4	75.8 ± 0.3	75.9 ± 0.4	75.7 ± 0.3	75.8 ± 0.4	75.8 ± 0.3
	KNN	81.9 ± 0.4	79.6 ± 0.4	85.1 ± 0.5	83.3 ± 0.4	86.4 ± 0.4	84.3 ± 0.4	87.6 ± 0.4	85.8 ± 0.4	87.1 ± 0.5	85.1 ± 0.4	85.4 ± 0.4	83.6 ± 0.4	82.8 ± 0.5	80.3 ± 0.4
	SVM	86.8 ± 0.5	84.9 ± 0.4	89.1 ± 0.4	87.4 ± 0.4	90.6 ± 0.4	88.8 ± 0.4	90.1 ± 0.4	88.4 ± 0.4	90.0 ± 0.4	88.3 ± 0.4	87.9 ± 0.4	85.9 ± 0.4	86.2 ± 0.4	83.8 ± 0.4

Table 3. *Cont.*

db8	DT	77.1 ± 0.5	76.0 ± 0.4	79.9 ± 0.4	78.1 ± 0.5	81.5 ± 0.4	79.1 ± 0.4	82.1 ± 0.5	79.9 ± 0.4	81.3 ± 0.4	79.3 ± 0.4	78.6 ± 0.4	76.4 ± 0.4	77.0 ± 0.5	75.9 ± 0.4
	NB	75.8 ± 0.4	75.8 ± 0.3	76.1 ± 0.4	75.9 ± 0.4	76.6 ± 0.4	75.8 ± 0.3	77.3 ± 0.4	75.9 ± 0.4	76.1 ± 0.4	75.8 ± 0.3	75.8 ± 0.4	75.7 ± 0.3	75.8 ± 0.4	75.7 ± 0.3
	KNN	81.3 ± 0.4	79.2 ± 0.4	84.4 ± 0.5	82.8 ± 0.4	85.8 ± 0.4	83.8 ± 0.4	87.0 ± 0.4	85.2 ± 0.4	86.4 ± 0.4	84.6 ± 0.4	84.8 ± 0.4	83.1 ± 0.4	82.2 ± 0.4	79.8 ± 0.4
	SVM	86.3 ± 0.5	84.4 ± 0.4	88.5 ± 0.4	86.9 ± 0.4	89.9 ± 0.4	88.2 ± 0.4	89.6 ± 0.4	87.9 ± 0.4	89.4 ± 0.4	87.8 ± 0.4	87.3 ± 0.4	85.4 ± 0.4	85.7 ± 0.4	83.3 ± 0.4
db9	DT	76.8 ± 0.5	76.0 ± 0.4	79.6 ± 0.4	77.8 ± 0.4	81.1 ± 0.4	78.8 ± 0.4	81.7 ± 0.5	79.6 ± 0.4	80.9 ± 0.4	79.0 ± 0.4	78.3 ± 0.4	76.2 ± 0.4	76.7 ± 0.5	75.8 ± 0.4
	NB	75.8 ± 0.4	75.7 ± 0.3	76.0 ± 0.4	75.9 ± 0.4	76.4 ± 0.4	75.8 ± 0.3	77.0 ± 0.4	75.8 ± 0.4	75.9 ± 0.4	75.7 ± 0.3	75.8 ± 0.4	75.7 ± 0.3	75.7 ± 0.4	75.7 ± 0.3
	KNN	80.9 ± 0.4	78.9 ± 0.4	83.9 ± 0.4	82.4 ± 0.4	85.3 ± 0.4	83.4 ± 0.4	86.5 ± 0.4	84.8 ± 0.4	85.9 ± 0.4	84.2 ± 0.4	84.3 ± 0.4	82.7 ± 0.4	81.8 ± 0.4	79.5 ± 0.4
	SVM	85.9 ± 0.5	84.1 ± 0.4	88.1 ± 0.4	86.5 ± 0.4	89.4 ± 0.4	87.8 ± 0.4	89.1 ± 0.4	87.5 ± 0.4	88.9 ± 0.4	87.4 ± 0.4	86.9 ± 0.4	85.1 ± 0.4	85.3 ± 0.4	83.0 ± 0.4
db10	DT	76.6 ± 0.5	75.9 ± 0.4	79.3 ± 0.4	77.6 ± 0.4	80.8 ± 0.4	78.6 ± 0.4	81.4 ± 0.5	79.4 ± 0.4	80.6 ± 0.4	78.8 ± 0.4	78.1 ± 0.4	76.1 ± 0.4	76.5 ± 0.5	75.8 ± 0.4
	NB	75.8 ± 0.4	75.7 ± 0.3	76.0 ± 0.4	75.9 ± 0.4	76.2 ± 0.4	75.7 ± 0.3	76.8 ± 0.4	75.8 ± 0.4	75.8 ± 0.4	75.7 ± 0.3	75.8 ± 0.4	75.6 ± 0.3	75.7 ± 0.4	75.7 ± 0.3
	KNN	80.6 ± 0.4	78.7 ± 0.4	83.5 ± 0.4	82.1 ± 0.4	84.9 ± 0.4	83.1 ± 0.4	86.1 ± 0.4	84.5 ± 0.4	85.5 ± 0.4	83.9 ± 0.4	83.9 ± 0.4	82.4 ± 0.4	81.5 ± 0.4	79.3 ± 0.4
	SVM	85.6 ± 0.5	83.9 ± 0.4	87.7 ± 0.4	86.2 ± 0.4	89.0 ± 0.4	87.5 ± 0.4	88.7 ± 0.4	87.2 ± 0.4	88.5 ± 0.4	87.1 ± 0.4	86.5 ± 0.4	84.8 ± 0.4	85.0 ± 0.4	82.8 ± 0.4

https://doi.org/10.3390/a19070572

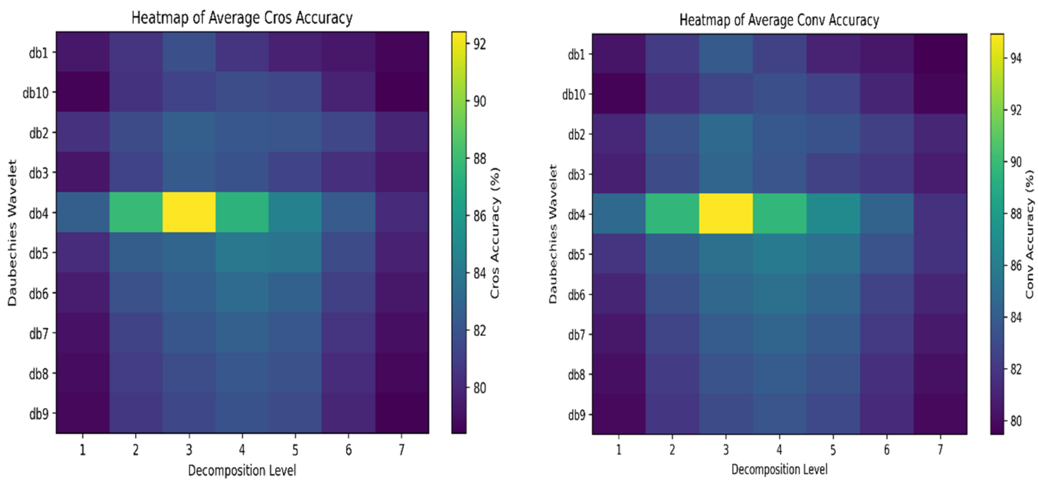

Figure 2. Heatmap of average accuracies for both Conv and Cross.

Table 4 presents a comprehensive performance evaluation of the four classifiers at the optimal db4 Level 3 configuration. The table demonstrates the accuracy, sensitivity, specificity, precision and F1-Score of the proposed framework. The Support Vector Machine (SVM) classifier appears to be the better architecture, achieving a maximum classification accuracy of 97.68 ± 0.64% with a higher F1-Score of 97.66%, which demonstrated its ability to balance precision and sensitivity in multi-state RUL classification. The high sensitivity rate of 97.82% and specificity rate of 97.45% for the SVM model shows a negligible rate of both false negative and false alarms, an important requirement for any industrial predictive maintenance system. K-Nearest Neighbors (KNN) stands as the second most reliable model with 95.98% classification accuracy, while the performance decline was observed in Decision Trees (DT) and Naive Bayes (NB), mainly in sensitivity which highlights the failure of simpler models to completely utilize the complex correlations within the wavelet transformed feature space. Furthermore, the low variation across all metrics, which ranges from ±0.48% to ±0.92%, highlights the stability and high generalizability of the toolkit, ensuring reliable RUL state predictions across the balanced dataset.

Table 4. Consolidated comparison.

Metric	SVM	KNN	DT	NB
Accuracy	97.68 ± 0.64%	95.98 ± 0.61%	94.01 ± 0.67%	92.28 ± 0.81%
Sensitivity	97.82 ± 0.55%	96.10 ± 0.72%	94.25 ± 0.68%	91.95 ± 0.92%
Specificity	97.45 ± 0.48%	95.75 ± 0.65%	93.60 ± 0.73%	92.70 ± 0.85%
Precision	97.51 ± 0.62%	95.82 ± 0.58%	93.85 ± 0.64%	92.41 ± 0.77%
F1-Score	97.66 ± 0.59%	95.96 ± 0.63%	94.05 ± 0.66%	92.18 ± 0.88%
Training Time (s)	1.84 ± 0.09	0.04 ± 0.01	0.12 ± 0.02	0.02 ± 0.01
Inference Time (ms/sample)	0.61 ± 0.05	0.3 ± 0.06	0.23 ± 0.02	0.09 ± 0.01

Figure 3 shows the confusion matrix for the SVM classifier with db4 wavelet and Level 3 decomposition feature set with conventional validation, in which 70% of the data was used to train the model, and the remaining 30% of the data was used for testing. The number of testing samples for each class was 300, in which for the 15% class 297 samples were correctly classified with 99% accuracy; for the 25% class 288 samples were correctly classified with 96% accuracy; for the 50% class 292 samples were correctly classified with 97.33% accuracy; for the 75% class 295 samples were correctly classified with 98.33%

accuracy; and for the 100% class 293 samples were correctly classified with 97.67% accuracy. There are 3 instances where the 15% class was misclassified, 12 instances where the 25% class was misclassified, 8 instances where the 50% class was misclassified, 5 instances where the 75% class was misclassified and 7 instances where the 100% class was misclassified.

SVM Confusion Matrix (Accuracy: 97.67%)

OUTPUT \ TARGET	15%	25%	50%	75%	100%	SUM
15%	297 19.80%	2 0.13%	1 0.07%	0 0.00%	0 0.00%	300 99.00% 1.00%
25%	6 0.40%	288 19.20%	0 0.00%	4 0.27%	2 0.13%	300 96.00% 4.00%
50%	1 0.07%	4 0.27%	292 19.47%	2 0.13%	1 0.07%	300 97.33% 2.67%
75%	0 0.00%	2 0.13%	1 0.07%	295 19.67%	2 0.13%	300 98.33% 1.67%
100%	1 0.07%	2 0.13%	4 0.27%	0 0.00%	293 19.53%	300 97.67% 2.33%
SUM	305 97.38% 2.62%	298 96.64% 3.36%	298 97.99% 2.01%	301 98.01% 1.99%	298 98.32% 1.68%	1465 / 1500 97.67% 2.33%

Figure 3. Confusion matrix for SVM classifier Using db4 Level 3 features.

The experimental results of this research, with 97.68 $\pm$ 0.64% maximum classification accuracy, represent a major improvement over most of the existing literature discussed in Table 3. When compared to the fundamental models used in bearing diagnostics, such as the self-organizing maps in [10] and MLP networks in [12], which reported a classification accuracy of approximately 85%, the present study with WPT-based SVM framework provides a nearly 13% improvement in classification accuracy. This difference suggests that the conventional style of using raw signals or basic spectral features is inadequate for multi-state RUL classification in bearings, whereas the present study which is based on optimized wavelet domain features successfully isolates the transient energy of degradation. To statistically validate the classification models' performance, a One-way ANOVA test was applied. The result of the ANOVA test shows that the model performance was statistically significant with $p < 0.05$. This statistical significance shows that the performance difference for the models is reasonable and not a result of random variation. To further quantify model reliability, 95% confidence intervals were computed from the repeated cross-validation results. The SVM classifier achieved an accuracy of 97.68 $\pm$ 0.64%, corresponding to a 95% confidence interval of approximately 97.04–98.32%, confirming the robustness and stability of the proposed framework.

To further evaluate the contribution of the sensors separately, feature sets from vibration signals and temperature signals were separately used for classification. Table 5 shows the classification accuracy obtained using temperature features only, vibration features only, and the combined temperature–vibration feature set for the four classifiers at the optimal db4 Level 3 configuration. The results show that vibration features provide better classification performance than temperature features for all classifiers, indicating that vibration signals contain the main information related to bearing degradation. For example, the SVM classifier achieved 92.1% accuracy using vibration features alone, while temperature features alone achieved 72.8% accuracy. However, the best results were obtained when both temperature and vibration features were combined. The SVM classifier achieved the highest accuracy of 97.68%, while similar improvements were observed for KNN, DT, and NB classifiers. These results show that temperature data provides additional information that complements the vibration data, leading to better separation of the RUL states and improved overall classification performance. To verify that the improvement in classification due to multi-modal fusion is statistically significant, a paired *t*-test was conducted on accuracy runs comparing vibration only versus vibration+ temperature feature sets for the SVM classifier. The test yielded t = 18.79 ($p < 0.0001$) with a Cohen's d of 8.85, confirming that the 5.58 percentage-point gain is highly significant and not due to random variation. From a practical point of view, K-type thermocouples are low-cost sensors that are already present in most industrial equipment for overheating protection. The hardware overhead is marginal and negligible, justifying the multi-modal approach for predictive maintenance applications.

Table 5. Contribution of temperature and vibration features to RUL classification performance (db4–Level 3).

Classifier	Accuracy in %		
	Vibration Only	Temperature Only	Vibration + Temperature
SVM	92.1 ± 0.8	72.84 ± 1.12	97.68 ± 0.64
KNN	90.4 ± 0.8	70.95 ± 1.08	95.98 ± 0.61
DT	88.2 ± 0.9	69.8 ± 1.1	94.01 ± 0.67
NB	86.0 ± 1.0	68.5 ± 1.2	92.28 ± 0.81

Public datasets such as the CWRU and IEEE PHM2012 were not used for comparison because these datasets contain only vibration data and the synchronized temperature data is not available for direct comparison. However, the same methodology (db4 and Level 3 decomposition with SVM classifier) adopted in this research was applied to the vibration data from the CWRU dataset. The maximum classification accuracy obtained was 88.58%, which is almost near the classification accuracy reported for vibration, also 92.1% in this study. A direct comparison of this study's results with the literature is not fair due to differences in the datasets, operating conditions, and evaluation protocols, hence only a comparison in classification accuracy was done. While specialized SVM models in [14,27] achieved an impressive classification accuracy of 94.4% and 96.74% respectively, they still fall short of our 97.68% threshold attained in the present study. The most vital difference lies in the feature extraction technique used; while [14] used standard time-domain statistical features and [27] used PCA on the raw measurement from various sensors, the present study identifies the optimal feature space combination at the third decomposition level of the db4 wavelet. This specific level effectively acts as filter which removes the high-frequency industrial noise that typically limits the performance of models like those utilized in [16], which reported a classification accuracy of only 78.74%. The Deep Convolutional Neural Networks used in [34] and hybrid LSTM models used in [35] reported low classification accuracy; however, the dataset and the operational conditions used are different from the present study. The proposed method achieves competitive performance compared with results reported in the literature without taking into account the varying operational conditions and the difference in dataset. Direct performance comparisons should be interpreted cautiously because datasets, fault categories, and evaluation protocols differ among studies. Also, this research primarily focuses on conventional machine learning methods which take less computational time instead of using advanced models such as Convolutional Neural Network (CNN), Long Short-Term Memory (LSTM), etc.

One of the most convincing aspects of this study is the decrease in classification error between adjacent RUL states. In the work of [17], a classification accuracy of 99% was reported for the "normal" class, but accuracy significantly decreased when attempting to distinguish between different RUL stages. In contrast, the present study's F1-Score of 97.66% and the standard deviation of ±0.64% confirm that the db4 Level 3 features preserve high discriminability even as the bearing health changes through different RUL states. While few previous works like [36,37] report high accuracies of 98.88% and 100% respectively, they often rely on smaller, highly controlled datasets or binary conditions such as normal and faulty classes. The implemented framework achieves better performance using a comprehensive and balanced dataset across five distinct RUL states in roller bearing, showing a more robust and scalable outcome for real-world industrial predictive maintenance where computational efficiency and multi-state precision are both equally important.

The experimental result of this research indicates the possibility of implementing an intelligent RUL state prediction system for roller bearings in real-time industrial conditions. Based on this study results, the chosen db4 wavelet and Level 3 decomposition feature set allows conventional classifiers like SVM to match with the performance of deep learning models. The high specificity rate of 97.45% and sensitivity rate of 97.82% achieved in classifying five RUL states in roller bearing suggest that the proposed framework is effective. The misclassification rate that frequently affects the industrial maintenance plan is lower in this study.

The proposed framework has several limitations which are discussed further in this section. First, the model was validated on an industrial dataset under controlled operating conditions; its performance under different industrial environments may vary. Second, the framework relies exclusively on handcrafted statistical features extracted from WPT coefficients, which may not capture all degradation patterns present in varying operating conditions. Third, while the inference time data in Table 4 indicates low computational cost, formal hardware benchmarking on edge devices has not been conducted. The total processing time per window for the optimal db4 Level 3 SVM configuration, including filtering, WPT decomposition, feature extraction, feature reduction, and classification, was 5.8 ± 0.5 ms, representing 3.6% of the available 160 ms processing budget and confirming real-time suitability. Future work will investigate adaptive feature extraction, validation on publicly available benchmark datasets, deep learning models and hardware deployment under varying operating conditions. In conclusion, the capability of this methodology to maintain low variance across a balanced dataset emphasizes its consistency, providing technicians with a mathematically grounded tool for predictive maintenance. In the future, studies could focus on additional sensor fusion such as load and motor speed to optimize the results further.

5. Conclusions

This research developed a framework for accurately classifying the Remaining Useful Life (RUL) state of roller bearings using Wavelet Packet Transform (WPT) and machine learning algorithms. The proposed framework improves the performance of RUL state classification in roller bearings by combining effective wavelet feature extraction with supervised learning models. Different Daubechies wavelets (db1–db10) and seven decomposition levels were analyzed to find the most suitable feature configuration. The results showed that the db4 wavelet with the 3rd level decomposition was the best feature set for classifying different RUL states in roller bearing. The chosen wavelet configuration provided better time-frequency information, which helped to identify early bearing fault signals. When applied with a Support Vector Machine (SVM) classifier, the proposed framework achieved a classification accuracy of 97.68 $\pm$ 0.64%, which was higher than the performance of other models such as K-Nearest Neighbor (KNN), Decision Tree (DT), and Naive Bayes. The confusion matrix results showed that the proposed feature set improved the separation between different RUL states and reduced classification errors between similar bearing health states. This demonstrates the capability of the framework for reliable roller bearing condition monitoring. This research validates that appropriately selected wavelet-based features improve the accuracy and reliability of predictive maintenance systems. The developed framework provides a practical and efficient solution for reducing unexpected failures and improving maintenance planning in rotating machinery.

Funding: This research received no external funding and the APC was funded by University of Technology Bahrain (UTB).

Data Availability Statement: Restrictions apply to the availability of these data. Data were obtained from GDR TECH Industry and are available from the author with the permission of GDR TECH Industry and University of Technology Bahrain (UTB).

Acknowledgments: The author would like to thank the management of GDR Tech Industry for providing the administrative support necessary to carry out data collection within their company. Gratitude is also extended to the University of Technology Bahrain for providing the facilities and technical support required to successfully complete this study.

Conflicts of Interest: The author declares no conflict of interest.

List of Abbreviations

PdM	Predictive Maintenance
WPT	Wavelet Packet Transform
PCA	Principal Component Analysis
SVM	Support Vector Machine
KNN	K-Nearest Neighbor
DT	Decision Tree
NB	Naive Bayes
RMS	Root Mean Square
RUL	Remaining Useful Life
K	Kurtosis
CF	Crest Factor
RE	Relative Energy
MT	Mean Temperature
SD	Standard Deviation
CNN	Convolutional Neural Network
LSTM	Long Short-Term Memory

References

1. Palaniappan, R. A Systematic Review of Remaining Useful Life Prediction in Roller Bearings Using Artificial Intelligence Techniques. *Informatica* **2026**, *50*, 323–334. [CrossRef]
2. Khan, M.A.; Asad, B.; Kudelina, K.; Vaimann, T.; Kallaste, A. The Bearing Faults Detection Methods for Electrical Machines—The State of the Art. *Energies* **2022**, *16*, 296. [CrossRef]

3. Abdalla, M.A.B.; Palaniappan, R.; Nataraj, S.K.; Noaman, N.M.; Vijean, V.; Nabi, F.G. An Overview of Industry 5.0: Key Features, Advantages, Limitations and Future Directions. In *Tech Fusion in Business and Society: Harnessing Big Data, IoT, and Sustainability in Business: Volume 1*; Hamdan, R.K., Ed.; Springer Nature: Cham, Switzerland, 2025; pp. 633–643.
4. Ji, A.; Woo, W.L.; Wong, E.W.L.; Quek, Y.T. Rail Track Condition Monitoring: A Review on Deep Learning Approaches. *Intell. Robot.* **2021**, *1*, 151–175. [CrossRef]
5. Zhang, J.; Chen, K.; Wu, F.; Qian, Q.; Huang, T.; Cheng, Y.; Yin, S. Remaining Useful Life Prediction Based on Self-Attention Mechanism -Sequential Variational Autoencoder: From a Semi-Supervised Perspective. *Adv. Eng. Inform.* **2026**, *71*, 104242. [CrossRef]
6. Landau, D.; de Pater, I.; Mitici, M.; Saurabh, N. Federated Learning Framework for Collaborative Remaining Useful Life Prognostics: An Aircraft Engine Case Study. *Future Gener. Comput. Syst.* **2026**, *174*, 107945. [CrossRef]
7. Babak, V.; Babak, S.; Zaporozhets, A. Stochastic Models of Diagnostic Signals Arising During the Operation of Electrical Equipment. In *Statistical Diagnostics of Electric Power Equipment*; Springer Nature: Cham, Switzerland, 2025; pp. 75–122.
8. Palaniappan, R. Predictive Manufacturing: State of the Art, Design Standards, Limitations, Challenges, and Future Perspectives. In *AIP Conference Proceedings*; AIP Publishing LLC: Melville, NY, USA, 2024; p. 020004.
9. Lu, Q.; Cheng, L.; Zhu, D.; Li, M. Fault Prediction Method towards Gearbox Based on Digital Twin and Deep Transfer Learning. *Eng. Res. Express* **2026**, *8*, 085506. [CrossRef]
10. Huang, R.; Xi, L.; Li, X.; Richard Liu, C.; Qiu, H.; Lee, J. Residual Life Predictions for Ball Bearings Based on Self-Organizing Map and Back Propagation Neural Network Methods. *Mech. Syst. Signal Process.* **2007**, *21*, 193–207. [CrossRef]
11. Chen, S.L.; Craig, M.; Callan, R.; Powrie, H.; Wood, R. Use of Artificial Intelligence Methods for Advanced Bearing Health Diagnostics and Prognostics. In *Proceedings of the 2008 IEEE Aerospace Conference*; IEEE: New York, NY, USA, 2008; pp. 1–9.
12. Castejón, C.; Lara, O.; García-Prada, J.C. Automated Diagnosis of Rolling Bearings Using MRA and Neural Networks. *Mech. Syst. Signal Process.* **2010**, *24*, 289–299. [CrossRef]
13. Sun, C.; Zhang, Z.; He, Z. Research on Bearing Life Prediction Based on Support Vector Machine and Its Application. *J. Phys. Conf. Ser.* **2011**, *305*, 012028. [CrossRef]
14. Kim, H.-E.; Tan, A.C.C.; Mathew, J.; Choi, B.-K. Bearing Fault Prognosis Based on Health State Probability Estimation. *Expert Syst. Appl.* **2012**, *39*, 5200–5213. [CrossRef]
15. Tian, Z. An Artificial Neural Network Method for Remaining Useful Life Prediction of Equipment Subject to Condition Monitoring. *J. Intell. Manuf.* **2012**, *23*, 227–237. [CrossRef]
16. Medjaher, K.; Tobon-Mejia, D.A.; Zerhouni, N. Remaining Useful Life Estimation of Critical Components with Application to Bearings. *IEEE Trans. Reliab.* **2012**, *61*, 292–302. [CrossRef]
17. Ben Ali, J.; Chebel-Morello, B.; Saidi, L.; Malinowski, S.; Fnaiech, F. Accurate Bearing Remaining Useful Life Prediction Based on Weibull Distribution and Artificial Neural Network. *Mech. Syst. Signal Process.* **2015**, *56–57*, 150–172. [CrossRef]
18. Ren, L.; Cui, J.; Sun, Y.; Cheng, X. Multi-Bearing Remaining Useful Life Collaborative Prediction: A Deep Learning Approach. *J. Manuf. Syst.* **2017**, *43*, 248–256. [CrossRef]
19. Deutsch, J.; He, D. Using Deep Learning-Based Approach to Predict Remaining Useful Life of Rotating Components. *IEEE Trans. Syst. Man Cybern. Syst.* **2018**, *48*, 11–20. [CrossRef]
20. Ren, L.; Sun, Y.; Wang, H.; Zhang, L. Prediction of Bearing Remaining Useful Life With Deep Convolution Neural Network. *IEEE Access* **2018**, *6*, 13041–13049. [CrossRef]
21. Cheng, C.; Ma, G.; Zhang, Y.; Sun, M.; Teng, F.; Ding, H.; Yuan, Y. A Deep Learning-Based Remaining Useful Life Prediction Approach for Bearings. *IEEE/ASME Trans. Mechatron.* **2020**, *25*, 1243–1254. [CrossRef]
22. Lu, B.-L.; Liu, Z.-H.; Wei, H.-L.; Chen, L.; Zhang, H.; Li, X.-H. A Deep Adversarial Learning Prognostics Model for Remaining Useful Life Prediction of Rolling Bearing. *IEEE Trans. Artif. Intell.* **2021**, *2*, 329–340. [CrossRef]
23. Bharatheedasan, K.; Maity, T.; Kumaraswamidhas, L.A.; Durairaj, M. Enhanced Fault Diagnosis and Remaining Useful Life Prediction of Rolling Bearings Using a Hybrid Multilayer Perceptron and LSTM Network Model. *Alex. Eng. J.* **2025**, *115*, 355–369. [CrossRef]
24. Vlachou, V.I.; Karakatsanis, T.S.; Vologiannidis, S.D.; Efstathiou, D.E.; Karapalidou, E.L.; Antoniou, E.N.; Efraimidis, A.E.; Balaska, V.E.; Vlachou, E.I. Intelligent Fault Diagnosis of Ball Bearing Induction Motors for Predictive Maintenance Industrial Applications. *Machines* **2025**, *13*, 902. [CrossRef]
25. Kumar, H.S.; Upadhyaya, G. Fault Diagnosis of Rolling Element Bearing Using Continuous Wavelet Transform and K- Nearest Neighbour. *Mater. Today Proc.* **2023**, *92*, 56–60. [CrossRef]
26. Motahari-Nezhad, M.; Jafari, S.M. Comparison of MLP and RBF Neural Networks for Bearing Remaining Useful Life Prediction Based on Acoustic Emission. *Proc. Inst. Mech. Eng. Part J J. Eng. Tribol.* **2023**, *237*, 129–148. [CrossRef]
27. Palaniappan, R. Comparative Analysis of Support Vector Machine, Random Forest and k-Nearest Neighbor Classifiers for Predicting Remaining Usage Life of Roller Bearings. *Informatica* **2024**, *48*, 39–52. [CrossRef]

28. Farooq, U.; Ademola, M.; Shaalan, A. Comparative Analysis of Machine Learning Models for Predictive Maintenance of Ball Bearing Systems. *Electronics* **2024**, *13*, 438. [CrossRef]
29. Lourari, A.W.; Benhedjouh, T. RUL Estimation of Rolling Element Bearings Using a Hybrid Wavelet Packet Decomposition–Recursive Feature Elimination–Adaptive Neuro Fuzzy Inference System Framework. *Int. J. Progn. Health Manag.* **2026**, *17*. [CrossRef]
30. Hua, Z.; Zheng, Z.; Pahon, E.; Pera, M.-C.; Gao, F. Lifespan Prediction for Proton Exchange Membrane Fuel Cells Based on Wavelet Transform and Echo State Network. *IEEE Trans. Transp. Electrif.* **2022**, *8*, 420–431. [CrossRef]
31. Tobon-Mejia, D.A.; Medjaher, K.; Zerhouni, N.; Tripot, G. Estimation of the Remaining Useful Life by Using Wavelet Packet Decomposition and HMMs. In *Proceedings of the 2011 Aerospace Conference*; IEEE: New York, NY, USA, 2011; pp. 1–10.
32. Dhungana, H.; Kampen, A.-L.; Lundervold, A.S.; Øvsthus, K. Remaining Useful Life Prediction of Rolling Bearings via Wavelet Feature Fusion and LSTM Networks. *Int. J. Adv. Manuf. Technol.* **2026**, *142*, 2913–2930. [CrossRef]
33. Nishat Toma, R.; Kim, J.-M. Bearing Fault Classification of Induction Motors Using Discrete Wavelet Transform and Ensemble Machine Learning Algorithms. *Appl. Sci.* **2020**, *10*, 5251. [CrossRef]
34. Ding, H.; Yang, L.; Cheng, Z.; Yang, Z. A Remaining Useful Life Prediction Method for Bearing Based on Deep Neural Networks. *Measurement* **2021**, *172*, 108878. [CrossRef]
35. Magadán, L.; Granda, J.C.; Suárez, F.J. Robust Prediction of Remaining Useful Lifetime of Bearings Using Deep Learning. *Eng. Appl. Artif. Intell.* **2024**, *130*, 107690. [CrossRef]
36. Yan, M.; Wang, X.; Wang, B.; Chang, M.; Muhammad, I. Bearing Remaining Useful Life Prediction Using Support Vector Machine and Hybrid Degradation Tracking Model. *ISA Trans.* **2020**, *98*, 471–482. [CrossRef] [PubMed]
37. Wang, Q.; Wang, S.; Wei, B.; Chen, W.; Zhang, Y. Weighted K-NN Classification Method of Bearings Fault Diagnosis with Multi-Dimensional Sensitive Features. *IEEE Access* **2021**, *9*, 45428–45440. [CrossRef]

https://doi.org/10.3390/a19070572